ELM crash theory: relaxation, filamentation, explosions and implosions

H.R. Wilson, J.W. Connor 1), S.C. Cowley 2), C.G. Gimblett 1), R.J. Hastie 1),
P. Helander 1), A. Kirk 1), S. Saarelma 1), and P.B. Snyder 3)

University of York, Heslington, York YO10 5DD UK
1) EURATOM/UKAEA Fusion Association, Culham Science Centre, Abingdon, Oxon OX14 3DB, UK
2) Imperial College, Prince Consort Road, London SW7 2BZ, UK, and UCLA, Los Angles, USA
3) General Atomics, PO Box 85608, San Diego, California, 94550

e-mail contact of main author: hw508@york.ac.uk

Abstract. The non-linear characteristics and consequences of ideal magnetohydrodynamic (MHD) instabilities relevant for the edge transport barrier region of tokamak plasmas are analysed theoretically. The focus is on two particular instabilities, the peeling mode and the ballooning mode, which are both thought to have an important role to play in Edge-Localised Modes (ELMs). The final state of the plasma edge after suffering a peeling mode is deduced by an extension of Taylor relaxtion theory. The model predicts the region of plasma affected by the instability which, when combined with the stored energy in this region, can be used to predict the energy expelled by the ELM. The result is consistent with measurements from Type III ELMs, for which the theory is thought to be most relevant. The ballooning mode, driven by the plasma pressure gradient, is thought to be important for larger ELMs. An analytic reduction of the fully non-linear ideal MHD equations reveals that the instability will cause the plasma to form filaments, which erupt explosively from the most unstable flux surface. A new result is that when the edge current density is low the filaments push into the core of the plasma. However, at higher current density, comparable to the bootstrap current in a low collisionality plasma, the filaments explode outwards to be ejected into the scrape-off layer and possibly beyond. If these filaments should strike the vessel wall in future, larger tokamaks such as ITER, they could do serious damage. This suggests that the edge current density will be an important control parameter.

1. Introduction

The standard operating regime for ITER is the high confinement H-mode. This high confinement is largely a result of a transport barrier that arises spontaneously at the plasma edge as the heating power is increased beyond a threshold. Steep pressure gradients build in this transport barrier, typically leading to high values of the bootstrap current there. Two types of instability can arise: ballooning modes driven by the pressure gradient and peeling, or kink, modes driven by the current density, or its gradient. These instabilities are now widely believed to be responsible for the so-called ELMs: edge-localised modes. These explosive events lead to a series of eruptions in which heat and particles are expelled from the plasma surface. The resulting heat loads are a major concern for ITER, both for the divertor area and the vacuum vessel wall.

While linear stability analysis has been tested rigorously against data at the onset of ELMs [1,2], this is insufficient to develop models for energy loss mechanisms. These will likely require a non-linear theory. In this paper, we address non-linear models for both peeling modes and ballooning modes. The focus is on the individual modes, employing analytic approximations to simplify the analysis and reveal their essential characteristics. In the following section, we address the peeling mode. We do not attempt to derive the detailed non-linear mechanisms here, but instead use a relaxation theory to predict the final state. The model, which we believe to be relevant for small Type III ELMs, provides a prediction for the ELM-affected region and the energy expelled during an ELM. Then, in Section 3, we address the non-linear evolution of the ballooning mode. We employ an expansion which is

rigorously valid in the early non-linear evolution. We predict that the ballooning mode causes filaments of plasma to be ejected from the most unstable flux surface, with an explosive growth rate even close to linear marginal stability. A new result is that the filaments are only ejected outwards, towards the vessel wall, provided there is sufficient edge current density. We close in Section 4 with a summary and discussion, considering the implications for ITER and future work necessary to model the ELM energy and particle loss.

2. A peeling mode/Taylor relaxation based ELM model

In this section we discuss a model for ELMs that is based on the idea that a toroidal peeling instability can trigger a Taylor relaxation [3] of the plasma edge region [4]. The tokamak is not generally thought of as a relaxing system: although there is excess potential energy in the equilibrium fields, it is not readily available simply because there are, in general, few active MHD modes to release it. The converse is true in the reversed field pinch where there is a wealth of modes which can continuously release equilibrium energy, giving rise to the so-called "dynamo" effect. Nevertheless, some regions of the tokamak, such as the core region (whenever $q_0 < 1$), will have modes available and this has formed the basis for a relaxation based theory of sawtooth behaviour [5]. Here we propose that because the tokamak edge is prone to ballooning and peeling modes, in particular when it has entered the "H-mode" of operation and steep equilibrium gradients have developed, a similar "relaxing plasma" view can be adopted for ELM activity. We will emphasise the role of peeling modes in this model (perhaps, then, best suited to describe Type III ELMs), and a simple argument serves to support this position. Edge pressure gradients give rise to the 'bootstrap' current, which for large aspect ratio is

$$\mu_0 J_B \sim -2\mu_0 \frac{\varepsilon_0^{1/2}}{B_p}\frac{dp}{dr} = \frac{B}{R_0}\frac{\alpha_B}{\varepsilon^{1/2}q} \qquad (1)$$

This current must be taken into account in any equilibrium calculation. Here we have defined the minor radius, r, the major radius R_0, inverse aspect ratio, $\varepsilon_0 = r/R_0$, the poloidal field B_p, the total magnetic field B, the safety factor q and the pressure p; α_B is a dimensionless measure of the pressure gradient. There are then implications for ballooning stability as can be seen by writing Ampère's law in the form $\mu_0 J = B_0(2-s)/R_0 q$, where s is the magnetic shear. If we assume that the total current J is solely the bootstrap current then it follows that $\alpha_B = \varepsilon_0^{1/2}(2-s)$. We see that the effect of the bootstrap current is to reduce the magnetic shear at high pressure gradient. Such low shear equilibria are generally less prone to ballooning modes due to access to the so-called second stability regime [6]. Indeed, ballooning instabilities can disappear completely for negative shear, corresponding to $\alpha_B > 2\,\varepsilon_0^{1/2}$.

The peeling mode is essentially an ideal kink mode driven by the differential torque caused by the presence of edge current density. We assume that when the peeling stability boundary is crossed there is a release of equilibrium energy leading to the formation of a relaxed state. This state is simply that of a flattened current density. For conventional, monotonically decreasing current profiles the edge current density would then be higher than the initial, un-relaxed state. By itself this effect would further destabilise the peeling mode. However, there is an additional effect caused by the relaxation: the formation of skin currents at the inner boundary of the relaxed region and at the plasma/vacuum interface, corresponding to $r=r_E$ and $r=a$ respectively. For conventional current profiles we find that the skin current at $r=a$ is *negative* (see Fig 1) with respect to the plasma current. This contributes a stabilising effect. At a critical value of r_E-a these effects compensate each other, while for lower
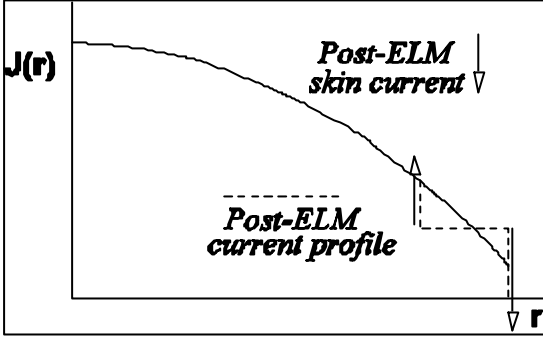
Figure 1: A schematic of the pre- (full) and post-ELM (dashed) relaxed current profiles showing the formation of skin currents

values the destabilising contribution dominates. Above the critical value of r_E-a, all peeling modes are stable, so we interpret this critical width as the ELM-affected region. Combining the width with the pressure gradient in this region provides us with an estimate of the ELM energy loss.

The first task in constructing our model is to calculate the relaxed state that is appropriate for an annular plasma region. This entails forming an extended version of the original Taylor calculation. We seek to minimise the annular magnetic energy and hypothesise that both the helicity of the annulus and the poloidal flux ψ are conserved. A simple calculation then gives the relaxed q profile (flat current) as $q=r^2/(Cr^2+D)$, where the coefficients C and D depend on the helicity and flux.

Starting from the force balance equation for the poloidal flux ψ

$$\frac{d}{dr}\left(r\frac{d\mathbf{y}}{dr}\right)-\frac{m^2\mathbf{y}}{r}=\mathbf{m}_0\frac{m}{F}\frac{dJ}{dr}\mathbf{y}$$

where $F=m(BR_0)(1/q-n/m)$, we introduce dimensionless quantities: $\Delta_X=(1/q_X-n/m)$, a measure of the 'distance' from the rational surface (located in the vacuum region), $K_X=\mu_0(R_0/B)I_{js}=[[1/q]]^{X+}_{X-}$, the jump in q due to the presence of a skin current at position $r=X$, and $\Delta'_X=[[(r/\psi)d\psi/dr]]$, the well-known MHD stability index.

Boundary conditions have to be applied at $r=r_E$, a and these conditions correspond physically to requiring that perturbed surfaces remain flux surfaces and that the tangential stress across the perturbed interfaces be continuous. With subscripts E and a referring to the inner and outer radii, we find the following system

$$\Delta_a\left[\Delta_a\Delta'_a+I_a\right]+K_a\left[\left(K_a-2\Delta_a\right)\left(\Delta'_a+m-1\right)-2\frac{n}{m}-I_a\right]=0 \tag{2}$$

$$\Delta_{E-}\left[\Delta_{E-}\Delta'_E+I_{E-}-I_{E+}\right]+K_E\left[\left(K_E-2\Delta_{E-}\right)\left(\Delta'_E+m-1\right)+2\frac{n}{m}-I_{E-}\right]=0 \tag{3}$$

$$\Delta'_E=-2m\frac{\left(\Delta'_a+2m\right)}{\left(g\Delta'_a+2m\right)} \tag{4}$$

where $g=1-(r_E/a)^{2m}$ and I_X is the local current density at position $r=X$ neglecting the skin currents. In deriving these equations we have taken solutions $\psi\sim r^{\pm m}$, appropriate for large m. The left hand side of Eq (2) is $\sim-\delta W$, the ideal MHD energy functional.

We examine the simple initial q profile $q_i=q_0+(q_a-q_0)r^2$, for $0\leq r\leq1$ and $q_i=q_a r^2$ for $r\geq1$. Then, for fixed q_0, q_a Eqs (2-4) yield a sequence of unstable (m, n) values (i.e. for which $\delta W<0$). Increasing $d_E=(a-r_E)/a$ we can then find a marginally stable state for each (m, n) pair. We assume that the final state corresponds to the maximum d_E.

Figure 2: The maximal marginal d_E, plotted against initial edge q_a value. The dashed curve gives an analytic approximation for d_E(max) in the case n=1.
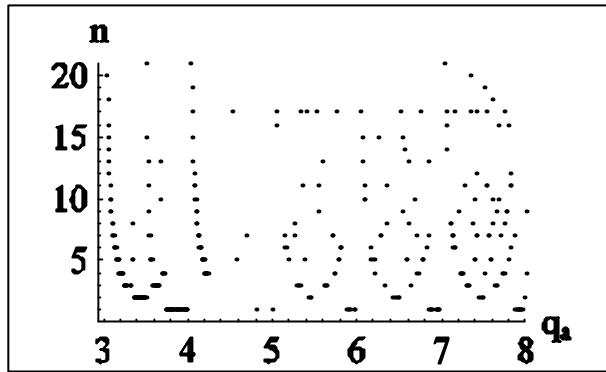
Figure 3: The toroidal mode numbers n that give the maximal marginal d_E values of Fig. 2, plotted against the initial edge q_a value.

Now, scanning in q_a with q_0=1 we can produce Figs 2 and 3, which show d_E(max) and the corresponding n values. An interesting feature of these figures is their "scatter" which can be traced to the precise rational m/n value that occurs. We see that the final stable states occupy ~10% of the minor radius. Figure 2 can be used, in combination with the toroidal peeling stability condition [7] to deduce the actual pressure energy lost in the relaxation. For example, for parameters typical of a collisional MAST edge plasma this gives $\Delta W_{\mathrm{ELM}}/W_{\mathrm{PED}}$ ~ few percent, which is in good agreement with experiment [8].

Future studies will include the bootstrap current in the calculation of the initial equilibrium, and an investigation of the subsequent development of the negative current sheet, which will be unstable to high m tearing modes.

3. Non-linear ballooning mode theory

A full 3-D numerical solution of the ideal MHD equations to derive the structure and evolution of modes having a long wave-length along the magnetic field lines and short wavelength perpendicular to them is extremely challenging. It is therefore useful to employ approximations that allow the full system to be reduced so that the essential properties of this type of instability can be deduced. This serves as an important benchmark for the large-scale non-linear simulations, and also helps us to interpret both experimental tokamak plasma and numerical data. We have previously reported such an analytic reduction, based on an expansion in the ratio of the perpendicular to parallel (to the magnetic field lines) wavelength, which is assumed to be small [9,10]. That result was valid for the range of Mercier stability index, $0>D_M>-3/4$ which is usually, but not always satisfied in the plasma edge. In that limit we found that the inertia is dominated by the plasma that is far along the erupting flux tube, *i.e.* far from the region of maximum displacement. This introduces a fractional time derivative into the equation describing the evolution of the flux tube in the directions perpendicular to the magnetic field line. We have recently extended this calculation to incorporate a regime relevant for stronger plasma shaping, when $D_M<-3/4$. This combines, in a single unified theory, the two previous theories derived in the two extreme limits [10,11]. The result is:

$$C_I \frac{\partial}{\partial \boldsymbol{a}} \frac{\partial^2}{\partial t^2}\left[\int_0^t dt' \frac{F(t')}{(t-t')^{l_S-l_L-1}}\right] + rC \frac{\partial}{\partial \boldsymbol{a}}\left(\frac{\partial^2 F}{\partial t^2}\right) = C_1\left[2(1-\boldsymbol{m})\frac{\partial F}{\partial \boldsymbol{a}} - C_0 \frac{\partial^2 u}{\partial \boldsymbol{y}^2}\right] + C_2 \frac{\partial F^2}{\partial \boldsymbol{a}} + C_4 \frac{\partial F}{\partial \boldsymbol{a}}\frac{\partial^2 \overline{F^2}}{\partial \boldsymbol{y}^2}$$

$$+ C_3\left[\left(\frac{\partial F}{\partial \boldsymbol{y}}\right)^2 - \frac{\partial^2 u}{\partial \boldsymbol{y}^2}\frac{\partial F}{\partial \boldsymbol{a}} - \frac{1}{2}\frac{\partial^2 \overline{F^2}}{\partial \boldsymbol{y}^2}\right]$$

(5)

where we have written the full 3-D solution for the amplitude of the perturbation in the form

$$\boldsymbol{x}(\boldsymbol{y},\boldsymbol{a},\boldsymbol{q};t) = F(\boldsymbol{y},\boldsymbol{a};t)H(\boldsymbol{q},\boldsymbol{ey})$$

and $F=\partial u/\partial\alpha$. The parameter μ is a measure of the ballooning drive, with $\mu<1$ corresponding to linear instability. Our coordinates are the poloidal flux, ψ, a field line label, α and a poloidal angle, θ, which measures the distance along the field line. The variation along the field line, $H(\theta,\varepsilon\psi)$, is the solution of the standard, linear ballooning equation. This is not assumed: it is derived from the ordering procedure that we employ. The dependence of H on ψ is due only to relatively slow equilibrium variations, as indicated explicitly by the introduction of the small ordering parameter, ε.

Notice that the inertia consists of the two terms on the left hand side of the equation. The first term represents the inertial contribution from the plasma far along the field line. It is a representation of a fractional time derivative, with an index equal to the difference between the two Mercier solutions, $\lambda=\lambda_S-\lambda_L=(1-4D_M)^{1/2}$. The second term is the inertia associated with the rest of the plasma, and has the second order time derivative expected from ideal MHD. The fractional derivative arises because far along the field line the amplitude decays at a rate which itself depends on the inertia. In linear theory, for example, the eigenfunction extends along the field line a distance which is inversely proportional to the growth rate. This means that the mass of plasma involved depends on the growth rate: multiplying this mass by the explicit quadratic dependence on growth rate results in a dependence of the total inertia which varies with growth rate as a fractional power.

Turning to the terms on the right hand side, the first two terms, linear in F and u, are simply the linear mode drives. The quadratic nonlinearity is the one responsible for the explosive behaviour. Balancing this non-linearity against the dominant inertial term, we deduce that

$$F \sim \begin{cases} \dfrac{1}{[t_0(\boldsymbol{a},\boldsymbol{y})-t]^l} & 1 < l < 2 \\[3mm] \dfrac{1}{[t_0(\boldsymbol{a},\boldsymbol{y})-t]^2} & l > 2 \end{cases}$$

The time of the explosion, t_0 depends on the initial conditions.

The third term on the right determines the mode structure. Balancing this with the quadratic nonlinearity, we predict

$$\frac{(\Delta\boldsymbol{y})^2}{\Delta\boldsymbol{a}} \sim \begin{cases} \dfrac{1}{[t_0(\boldsymbol{a},\boldsymbol{y})-t]^l} & 1 < l < 2 \\[3mm] \dfrac{1}{[t_0(\boldsymbol{a},\boldsymbol{y})-t]^2} & l > 2 \end{cases}$$

This predicts that the mode tends to broaden radially, but narrow in the flux surface (perpendicular to the field line). Combined with the long wavelength behaviour along the field line, contained in the ballooning solution H, this therefore describes a filamentary structure, exploding from the flux surface that is most unstable to the ballooning mode. Such structures have been observed both in large scale

numerical simulations [12] and experimentally during the ELM [13]. The final terms complicate this picture, but are zero for up-down symmetric plasmas. Their effect will be assessed numerically in the future.

One can envisage a number of models for the resulting heat loss triggered by this instability [14]. One such model suggests that the filament remains attached to the pedestal on the inboard side, but pushes out into the scrape-off layer on the outboard side, possibly involving a reconnection as the filament pulls through the X-point. In this model, the filament acts as a conduit, through which hot plasma flows from the pedestal region into the SOL, or divertor region. The resulting model for the maximum heat loss that could occur in this process would require three ingredients: the flow rate of plasma and heat through the filament; the cross-sectional area of the filament, and the lifetime of the filament. Such a model, with input from experimental data, is able to produce trends seen in experimental databases [15]. It is clearly desirable, for a predictive model, to provide theoretical estimates for the inputs. This provides the motivation for our present work, which aims to calculate the coefficients appearing in Eq (5) and predict filament sizes for real experimental equilibria.

We have focussed on the coefficient of the quadratic non-linearity, C_2, which is

$$C_2 = \langle HP \rangle \tag{6}$$

$$HP = -(\underline{e}_\perp \cdot \nabla)Q + 2Q\frac{(\underline{e}_\perp \cdot \mathbf{?})}{B^2} + [(\underline{e}_\perp \cdot \nabla)\underline{H}] \cdot (\underline{B} \cdot \nabla)[(\underline{B} \cdot \nabla)\underline{H}] - \frac{1}{2}(\underline{e}_\perp \cdot \nabla)|(\underline{B} \cdot \nabla)\underline{H}|^2$$

$$+ \frac{1}{2B_0}[(\underline{H} \cdot \nabla)\underline{H}] \cdot \nabla a \, [\underline{e}_\wedge \cdot L(H\underline{e}_\perp)]$$

$$Q = \frac{1}{2}\Big[\underline{H} \cdot (\underline{B} \cdot \nabla)[(\underline{B} \cdot \nabla)\underline{H}] - |(\underline{B} \cdot \nabla)\underline{H}|^2\Big]$$

The vector $\boldsymbol{H}$ is the solution to the linear ballooning equation, including the perturbation parallel to the magnetic field, $\boldsymbol{e}_\perp$ and $\boldsymbol{e}_\wedge$ are vectors in the directions $\boldsymbol{B} \times \tilde{\mathbf{N}}\alpha$ and $\boldsymbol{B} \times \tilde{\mathbf{N}}\psi$ respectively, and $L(H\boldsymbol{e}_\perp)$ is related to the ideal MHD linear force operator (see [10]). One challenge is immediately apparent: calculation of this coefficient requires high order derivatives of the ballooning solution, $\boldsymbol{H}$, both along and across field lines. We therefore need to specify the equilibrium to higher accuracy than is typically possible from experimental equilibria. The procedure we follow is therefore the following.

1. We first scan the reconstructed equilibrium to deduce the most linearly unstable flux surface (to ballooning modes). We shall refer to this as the "reference" surface.
2. We then smooth this flux surface by performing a Fourier expansion in poloidal angle of the major radius, R, the vertical height, Z, and the poloidal field B_p.
3. To evaluate derivatives with respect to the poloidal flux requires two more flux surfaces, infinitesimally close to this one, and also smooth. It would be wrong to take two flux surfaces from the equilibrium solver and Fourier decompose these also: the three flux surfaces would then not satisfy the Grad-Shafranov equation to sufficient accuracy. Instead we use the expansion procedure of Mercier and Luc (*e.g.* see [15] to solve the Grad-Shafranov equation analytically in the vicinity of our reference flux surface. Thus, we are able to derive R, Z and B_p on these adjacent flux surfaces in terms of R, Z and B_p (and their poloidal derivatives) on the reference surface. The pressure and current profile functions are also required, of course.
4. We now perform a ballooning analysis on all three surfaces, allowing us to derive the required derivatives to high accuracy.

One advantage of the above procedure is that one can map out a large parameter space without re-calculating the equilibria. One can simply adjust the local pressure gradient and current density on the reference flux surface and the side-band flux surfaces, properly calculated, will automatically satisfy the Grad-Shafranov equation. This is the same principle as that employed analytically for generating $s-\alpha$ diagrams to illustrate the general features of linear ballooning mode stability, for example.

The second complication is associated with the integrand. This only decays as $\theta^{-\lambda}$, where $\lambda \sim 1.1$ is typical. To derive the integral along the field line to infinity would therefore require us to integrate out to an impractically large distance, as it would only converge very slowly $\sim\theta^{1-\lambda}$. It is therefore necessary to perform a two length scale analysis, valid as $|\theta|\rightarrow\infty$, and derive the asymptotic form of the integral analytically, matching to the numerical solution at lower θ.

We show here some first results from such an analysis. We take an equilibrium solution corresponding to a JET-like plasma with a relatively wide edge pedestal in the pressure. The flux surfaces towards the edge of the plasma (ie those analysed) are shown in Fig 4, where the red, dashed surface is the most unstable one (see Fig 5). The current for the equilibrium is held low to ensure that the ballooning mode forms a pressure gradient limit, and there is no access to second stability. Following the steps 1-4 above, we then evaluate C_2, with the surprising result that it is negative. This corresponds to plasma filaments erupting from the reference surface, but penetrating in towards the centre of the plasma, rather than out into the scrape-off layer as we originally anticipated. This, of course, would be good news for ITER as the filaments would then not strike the vessel wall. The result is, however, clearly at odds with the results of numerical simulations and experimental evidence, which do observe filaments erupting out into the scrape-off layer.
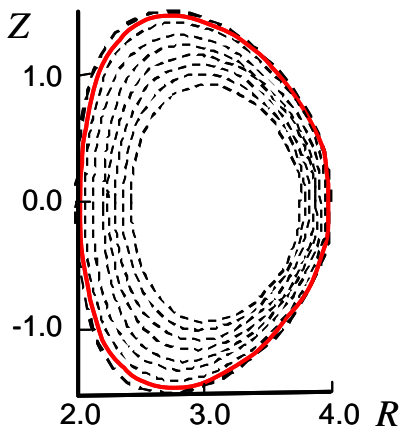
Figure 4: Flux surfaces of the equilibrium analysed. The full, red curve is the most unstable flux surface
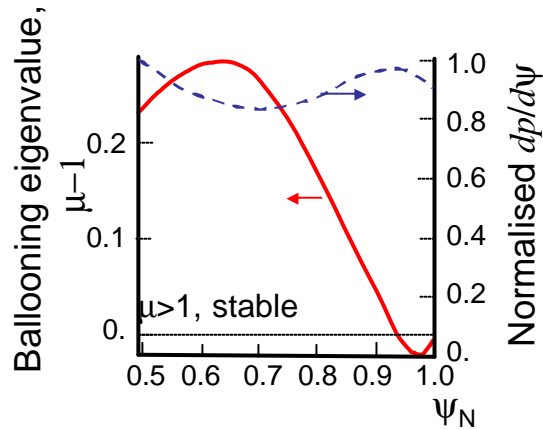
Figure 5: Ballooning eigenvalue as a function of normalised flux (unstable when it is negative). The dashed curve shows the normalised pressure gradient.

We know from experiment that the current density in the pedestal seems to have a significant effect on the ELM size. We therefore explore the effect of varying current density and pressure gradient on the value of C_2. The results are shown in Fig 6. Note that our analysis is only valid provided we are close to the linear marginal stability curve. From this figure we see that if a critical current is exceeded, C_2 switches sign and the filaments are then predicted to explode outwards into the scrape-off layer. More studies are required to explore whether this is a general result and to make quantitative comparisons with simulations and experiment. Given the complexity of the calculations, it is also desirable to build a physical picture of what is happening, and what determines whether the filaments propagate outwards or inwards. This is work in progress.
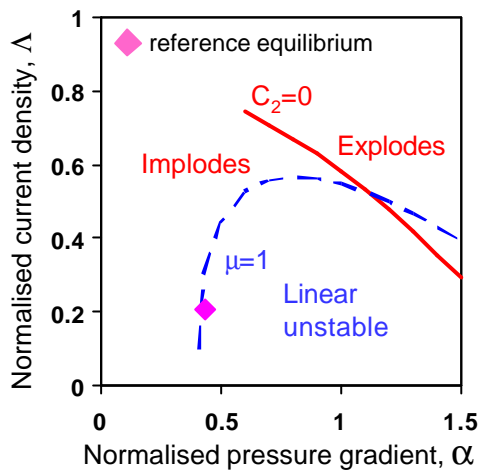
Figure 4: Contours of C₂=0 (full) and the marginally stable ballooning curve as pressure gradient and current are

4. Summary

We have described two non-linear theories for how ELMs could affect the tokamak pedestal. For peeling modes, we have described a relaxation theory, which is expected to be most relevant for small ELMs and the predicted energy loss is consistent with measurements from MAST. For the ballooning modes, we have found that a critical pedestal current density needs to be achieved in order for the filaments to be ejected outwards. Further work is required to explore whether this is qualitatively consistent with numerical simulations and experimental data. In particular, we would like to explore other equilibria to see if this is a robust result. Our result suggests that identifying a technique to control the current in the plasma edge may be important for controlling ELMs and protecting the vessel wall in future tokamaks such as ITER.

REFERENCES
[1] P.B. Snyder, et al, Phys. Plasmas **9** (2002) 2037
[2] S. Saarelma, et al, Plasma Phys. Control. Fusion **47** (2005) 713
[3] J B Taylor, Rev Modern Phys **58** (1986) 741
[4] C G Gimblett, R J Hastie and P Helander, Phys Rev Lett **96** (2006) 035006
[5] C G Gimblett and R J Hastie, Plasma Phys Control Fusion **36**, (1994) 1439
[6] J W Connor and R J Hastie, Phys Plasmas **11** (2004) 1520
[7] J W Connor, R J Hastie, H R Wilson and R L Miller, Phys Plasmas **5** (1998) 2687
[8] A. Kirk et al, Plasma Phys Control Fusion **46** (2004) A187
[9] S.C. Cowley et al, Plasma. Phys. Control. Fusion **45** (2003) A31
[10] H.R. Wilson and S.C. Cowley, Phys. Rev. Lett. **92** (2004) 175006-1
[11] O A Hurricane, et al, Phys Plasmas **4** (1997) 3565
[12] P.B. Snyder, H.R. Wilson and X.Q. Xu, Phys. Plasmas **12** (2005) 056115-1
[13] A. Kirk et al, Phys. Rev. Lett. **96**, (2006) 185001
[14] H.R. Wilson, et al Plasma Phys. Control. Fusion **48** (2006) A71
[15] A. Kirk, et al, This conference, paper EX/9-1
[16] R.L. Miller, et al Phys. Plasmas **5** (1998) 973